Simulation of Crude Oil Transportation with Drag Reduction Agents Using k-ϵ and k-ω Models

Ali Nasir Khalaf[1,*] and Asaad A. Abdullah[2]

[1]*Department of Chemical Engineering, College of Engineering, University of Basrah, Iraq*
[2]*Department of Materials Engineering, College of Engineering, University of Basrah, Iraq*
E-mail: alinasiralmajed@gmail.com
[*]Corresponding Author

Abstract

This work explores the possibility of using Newtonian turbulence $k - \epsilon$ and $k - \omega$ models for modelling crude oil flow in pipelines with drag reduction agents. These models have been applied to predict the friction factor, pressure drop and the drag reduction percentage. The simulation results of both models were compared with six published experimental data for crude oil flow in pipes with different types of drag reduction agents. The velocity near the wall was determined using the log law line of Newtonian fluid equation and by changing the parameter ΔB to achieve an excellent agreement with experimental data. Simulated data for $k - \epsilon$ model shows better agreement with most experimental data than the $k - \omega$ turbulence model.

Keywords: Crude oil, simulation, turbulence models, drag reduction, newtonian fluid.

1 Introduction

When crude oil flows in a pipe in turbulent flow, the friction factor decreases by using mall amount of an additive (drag reduction agents [DRA]). This addition is beneficial because it can decrease pumping energy requirements. Some current applications in which the drag reduction (DR) has been applied include oil transmission pipelines. DRAs are injected into pipelines in parts per million (ppm) to reduce turbulence and frictional losses in pipelines and improve throughput [1]. Several attempts in the literature range from experimental-based empirical correlations to complete numerical models for estimating the friction factor, pressure drop, and DRs in crude oil flow with DRAs. Most researchers conducted various field studies to understand the effects of DRAs. The majority of the results shared were found to be satisfactory in terms of how the DRA managed to increase the flow and overall throughput of the tested pipelines. M. H. Hassanean [2] found that the capacity of the production pipeline he tested was increased by 38% as a result of a reduced pressure drop of 36% due to DRA injection. Vejahati [3] developed a simple correlation which included the effect of all discounted factors in terms of the Reynolds number, polymer concentration, pipe diameters and crude oil properties.

Furthermore, Anees A. Khadom [4] examined the addition of polymeric DRAs on Iraqi crude oil pipelines and the effects of polymer concentration, pipe diameter, flow rate of pipeline and other factors. An important result of that work is the confirmation of the significant effect of the DRA in reducing the drag by approximately 50% with 50 ppm of polyacrylamide concentration. Various investigations have also investigated DR parameters such as pipe diameter, DRA concentration, flow rate, and temperature when using DRA for crude oil pressure reduction [5–8].

Software technology growth drives scientists to pay more attention to numerical approaches. One method of numerical analysis of turbulent DR flow is direct numerical simulation (DNS). Given that DNS tests can reliably display all the flow characteristics, certain numerical simulations such as averaged the Reynolds Navier Stokes (RANS) model can be validated for simulating turbulent flow with DRAs. Leighton et al. [9] were the first to introduce the RANS method. Recent years revealed an increasing interest in developing turbulence models for the prediction of the effects of DRAs.

Drag reduction can be defined as the increase in the pumping ability of a fluid, which is caused by addition of small amount of chemical additives. Therefore, during drag reduction and a given bulk mean velocity the fluid

with additive requires a lower pressure gradient to move than the fluid without additives. The main objective of drag reducing fluid research is to develop a viscoelastic turbulence model which can correctly calculate the mean velocity profile and drag reduction percentage (%DR) in all drag reduction regions and for any polymer solution. Rabie et al. [10] proposed a new DR flow model on the basis of the FENE-P (Finitely Extensible Nonlinear Elastic-Peterlin) theory. Finite element equations on the basis of the $k - \epsilon$ model were developed by Pinho et al. [11] for which turbulent correlation was applied. The Low Reynolds model was also proposed Resende et al. [12] for the estimation of the friction factor and DR. In the medium and low drag reduction percentage (%DR of up to 50%), the model can be tested by direct numerical simulation. The findings shown an improvement to the low DR model of Pinho et al. Using FLUENT software, Zheng et al. [13] obtained reliable outcomes by simulating turbulent DR flows via a user defined function (UDF).

Different aspects of DR and complex phenomena can be ascertained experimentally. Researchers who have exhibited interest in the experimental analysis of this field include [14–20]. Xin Zhang et al. [21] developed an analytical expression to predict the maximum limit of the DR percentage (%DR) in turbulent pipe flow with polymer additives. The model is based on the classic Navier-Stokes equation and the FENE-P theory. The aim of this work is to establish a model that facilitates the implementation of simulation calculations depending on several parameters such as pipe diameter, fluid velocity and DRA concentration. Two turbulence models were chosen, namely the low Reynolds number $k - \epsilon$ and $k - \omega$. Simulation results of both models were compared with six published experimental data for crude oil flow in pipes with different types of DRAs.

2 Numerical Modeling

The $k - \epsilon$ and $k - \omega$ models are two of the most common models in simulating fluid dynamics for turbulent and laminar flow in pipes and channels. Both models consist of two partial differential equations in the transport of kinetic energy (k) and turbulent energy dissipation (ϵ). These models are based on the continuity and the average RANS equations. The two partial differential transport equations are solved, in addition to the mass conservation and the equation of the momentum transfer equation. The $k - \epsilon$ and $k - \omega$ models are defined by the following equations [22].

2.1 Mean Flow Equations

Mass conservation:

$$\frac{\partial U_j}{\partial x_j} = 0 \tag{1}$$

Momentum conservation:

$$\rho \left[\frac{\partial U_i}{\partial t} + U_j \frac{\partial U_i}{\partial x_j} \right] = -\frac{\partial P}{\partial x_i} + \frac{\partial}{\partial x_j} \left[(\mu + \mu_T) \left(\frac{\partial U_i}{\partial x_j} + \frac{\partial U_j}{\partial x_i} \right) \right] \tag{2}$$

$\epsilon - \varepsilon$ **model transport equations.**

$$\rho \frac{\partial k}{\partial t} + \rho U_j \frac{\partial k}{\partial x_j} = \sigma_{ij} \frac{\partial U_i}{\partial x_j} - \rho \varepsilon + \frac{\partial}{\partial x_j} \left[\left(\mu + \frac{\mu_T}{\sigma_k} \right) \frac{\partial k}{\partial x_j} \right] \tag{3}$$

Turbulence dissipation equation:

$$\rho \frac{\partial \varepsilon}{\partial t} + \rho U_j \frac{\partial \varepsilon}{\partial x_j} = C_{\varepsilon 1} \frac{\varepsilon}{k} \sigma_{ij} \frac{\partial U_i}{\partial x_j} - C_{\varepsilon 2} \rho \frac{\varepsilon^2}{k} + \frac{\partial}{\partial x_j} \left[\left(\mu + \frac{\mu_T}{\sigma_\varepsilon} \right) \frac{\partial \varepsilon}{\partial x_j} \right]. \tag{4}$$

with $C_{\varepsilon 1} = 1.44$, $C_{\varepsilon 2} = 1.92$, $C_\mu = 0.09$, $\sigma_k = 1.0$, $\sigma_\varepsilon = 1.3$ and turbulent viscosity $\mu_T = \rho C_\mu \frac{k^2}{\varepsilon}$.

k − ω **model transport equations.**

Turbulence energy equation:

$$\rho \frac{\partial k}{\partial t} + \rho U_j \frac{\partial k}{\partial x_j} = \sigma_{ij} \frac{\partial U_i}{\partial x_j} - \beta^* \rho k \omega + \frac{\partial}{\partial x_j} \left[(\mu + \sigma_\omega{}^* \mu_T) \frac{\partial k}{\partial x_j} \right]. \tag{5}$$

Specific dissipation rate equation (the ω-equation):

$$\rho \frac{\partial \omega}{\partial t} + \rho U_j \frac{\partial \omega}{\partial x_j} = \alpha \frac{\omega}{k} \sigma_{ij} \frac{\partial U_i}{\partial x_j} - \beta \rho \omega^2 + \frac{\partial}{\partial x_j} \left[(\mu + \sigma_\omega \mu_T) \frac{\partial \omega}{\partial x_j} \right], \tag{6}$$

With

$$\alpha = \frac{5}{9} \cdot \beta = \frac{3}{40} \cdot \beta^* = \frac{9}{100} \cdot \sigma_\omega = \frac{1}{2} \cdot \sigma_\omega{}^* = \frac{1}{2} \cdot \mu_T = \rho \frac{k}{\omega}.$$

The equations of the two models are defined in Wilcox, but note that in 2006 the $k - \omega$ model was revised and improved [23]. However, in the software package used only for this work, the simulation option involved the earlier (standard) version of the $k - \omega$ model.
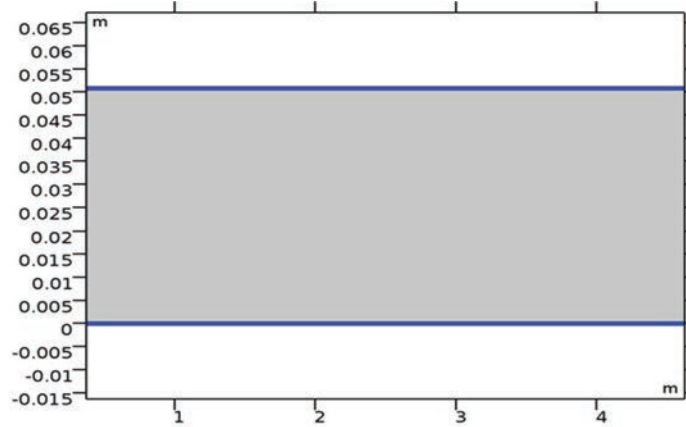
Figure 1   Computational domain.

2.2 Computational Domain and Boundary Conditions

A two-dimensional computational domain was used to simulate crude oil flow in a horizontal pipe as shown in Figure 1. The domain includes one inflow at the left side and one outflow at the right of the domain, while the pipe wall boundaries are located at the bottom and the top of the rectangular domain. Because we are investigating a fully developed flow, the flow only depends on the distance from the centerline of the pipe, R, and the position along the pipe, L.

For the two models, simulations performed in this work using the same mesh type and dimension for all computation runs. Later, with 59194 triangular elements for the fluid domain and 22644 quadrilateral elements on the pipe wall, much better results were obtained with an adaptive solver (with adaptive mesh refinement).

3 Drag Reduction Modeling in Pipes

As the near-wall field is influenced by fluid viscosity, the fluid velocity is zero at the pipe wall. The wall function approach ignores the flow field in the buffer layer and analytically computes a nonzero fluid velocity at the wall region. The layer above the pipe wall is called the viscous sublayer, and the second layer is the buffer layer. Viscous sublayer with turbulent stresses control viscous stresses. Moreover, the average turbulent flow velocity computed by the log-law region at a certain point is related to the wall distance by the logarithm expression in Figure 2.
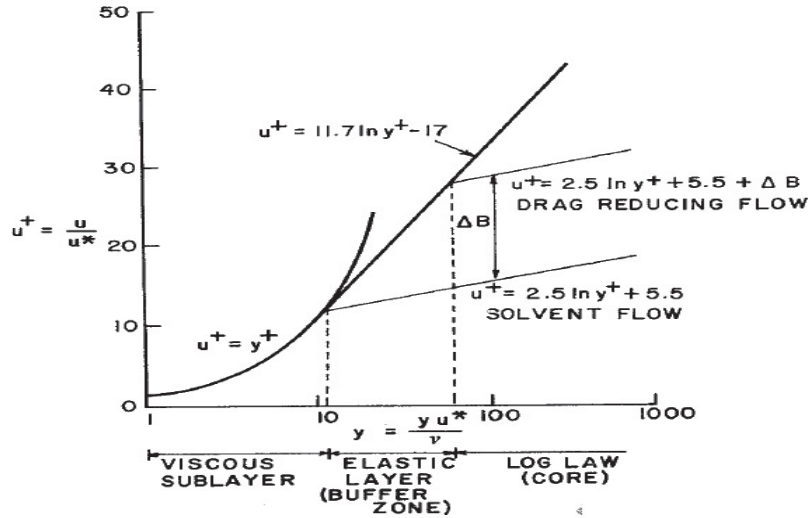
Figure 2   Velocity distribution in the boundary layer for polymer drag reduction based on typical velocity profile model for turbulent flow (from Sillin et al. Ref. 30).

Virk [24] experimentally found that the velocity distribution of a turbulent polymer solution flow in a pipe can be defined as the equation used for Newtonian flow (see Equations (7) and (8)) but with some velocity increment ΔB. When the DR value increases, the log law line of the Newtonian fluid is shifted by ΔB in the buffer layer region and the slope of the line is unchanged. For Newtonian fluids, the mean velocity profile can be expressed as [25].

$$u^+ = y^+ \quad y^+ \leq 11 \quad \text{sub layer region} \tag{7}$$

$$u^+ = 2.5 \ln y^+ + 5.5 \quad y^+ > 11.6 \quad \text{buffer layer region} \tag{8}$$

$$u^+ = 2.5 \ln y^+ + 5.5 + \triangle B \quad \text{flow with drag reduction agent} \tag{9}$$

Where $u^+ = \frac{U}{U^*} \cdot y^+ = \frac{U^* y}{\nu}$, y is the distance from the pipe wall, u is the stream velocity, U^* is the friction velocity, ν is the fluid kinematic viscosity. and ΔB is a dimensionless constant represents the effect of drag reduction as shown in Figure 1. Benzi et al. [26] found the following expression to calculate the constant ΔB if the constant 5,5 is replaced with 6.13:

$$\Delta B = 9.4 \ln(1 + \xi^3 N_P^3 C). \tag{10}$$

Where C is the polymer concentration in volume, ξ is the effective monomer hydrodynamic radius and Np is the degree of polymerization. Yang

et al. [27–29] investigated turbulent fluid flows in open channels and pipes with and without polymer additives. The mean velocity equations, root mean velocity fluctuation square and energy spectrum were developed by using the viscoelasticity of non-Newtonian properties model and the drag parameter (D*) on the basis of the modified Prandtl–Karman model Equation (9). The drag reducing properties of the linear polymer polyethylene oxide in turbulent flow was investigated by Xin Zhang et al. [30]. They developed a correlation for predicting %DR using Weissenberg (We), a dimensionless number that is related to polymer relaxation time and the concentration of the dilute solution. The physical nature of the polymer relaxation time and the difference between the diluted and semi-diluted polymer solutions is described. This current work investigates the performance of the two models $k - \epsilon$ and $k - \omega$ by using the finite element program COMSOL Multiphysics5.3a [31]. The turbulent flow in a pipe was simulated by solving Equations (1–6) to obtain the axial velocity profile, pressure drop and friction factor. The velocity near the wall was determined using Equation (9) and by changing parameter ΔB to achieve an excellent agreement with experimental data.

4 Methodology

At the end of each simulation run, a post-processing step is performed to compare the simulation results with the experimental data from the literature. The assumptions made in this work are as follows: (i) incompressible flow; (ii) steady state flow inside the horizontal pipe, with no fittings and elevation.; (iii) crude oil flow was under isothermal condition.

4.1 Prediction of Mixture Viscosity and Density

The density of a mixture from crude oil and drag reduction agent is calculated by [32].

$$\rho_{mix} = V_o\rho_o + V_s\rho_s \tag{11}$$

$$V_o = \frac{\rho_o}{\rho_o + \rho_s\left(\frac{1}{W_s} - 1\right)} \tag{12}$$

Or

$$W_s = \frac{V_s\rho_s}{V_s\rho_s + \rho_o(1 - V_s)} \tag{13}$$

where V_o, V_s, are the volume fraction for the oil (o) and the solvent or drag reduction agent (s) respectively and Ws is the weight fraction of solvent or DRA.

4.1.1 Crude Oil and Light Hydrocarbon Mixture

In literature, many models for heavy oil diluted with hydrocarbon solvents are documented to determine the viscosity of the mixture. With the exception of the model of Lederer all models varied considerably and failed to show a good agreement with experimental data [33]. Lederer [34] suggested a new model according to the standard form of the Arrhenius term to describe the viscosity of light hydrocarbon heavy oils or bitumen.

$$\log \mu_{mix} = \left(\frac{\alpha \, V_o}{\alpha \, V_o + V_s} \right) log\mu_o + \left(1 - \frac{\alpha \, V_o}{\alpha \, V_o + V_s} \right) log\mu_s \qquad (14)$$

where V_o, V_S, μ_o, μ_s are the volume fraction and viscosity of the oil (o) and solvent (s), respectively, and α is an empirical constant that varies from 0 to 1. The α parameter can be set with a least-square method approach to 0.4180. Shu [35] identified a common expression of α that can represent the viscosity of heavy oils or diluted bitumen. This parameter is related to the viscosity ratio and solvent and heavy oil densities

$$\alpha = \frac{17.04(\rho_o - \rho_s)^{0.5237} \, \rho_o{}^{3.237} \rho_s{}^{1.6316}}{\ln \left(\frac{\mu_o}{\mu_s} \right)} \qquad (15)$$

4.1.2 Crude Oil and Other Solvents Mixture

Heavy crude oil is blended with a solvent or diluent to achieve a certain viscosity. The viscosity of a crude oil blend therefore depends on the mass or volume of each portion of the blend and their viscosity. Mixture viscosity estimation presents a challenge, and different mixing rules are proposed in the literature for viscosity estimation. The viscosity of a crude oil mixture with diluents has been expressed in a new correlation by Saeed Mohammadi, et al. [36]. In their work, they collected various data for solvents and dilatants in the literature and determined an adjustable parameter using a genetic algorithm approach on the basis of 850 experimental data points. The developed model is given by:

$$\nu_{mix} = 0.011\exp \left(\frac{831.839}{LX} \right) \qquad (16)$$

$$LX = \sum_{i=1} w_i LX_I + 0.2C \tag{17}$$

$$C = \ln\left(\frac{v_j}{v_i}\right) \tag{18}$$

$$LX_i = \frac{831.839}{\ln\left(\frac{v_i}{0.01}\right)} \tag{19}$$

Where ν_{mix} and v_i are the kinematic viscosity of the mixture and the component in C.st and j stands for the most viscous component in the mixture.

4.2 Prediction of Friction Factor and Drag Reduction Percentage

Two steps were involved in the solution procedure. The first step was to solve the momentum and transport equations. The outputs from each simulation run indicate the pressure drop and velocity profile along the pipe. The second step compares the results of the friction factor and the Reynolds number with a set of experimental results of different crude oil DRAs as listed in Table 1.

The following values are computed:

Average velocity

$$u_{avg} = \frac{1}{\pi R^2} \int_0^R u \cdot 2\pi r \; dr \tag{20}$$

$$R_e = \frac{\rho_{mix} u_{avg} D}{\mu_{mix}} \tag{21}$$

$$f_{crude \; oil} = \frac{D \triangle P}{2\rho_{crude \; oil} L u_{avg}{}^2} \tag{22}$$

$$f_{with \; DRA} = \frac{D \triangle P}{2\rho_{mix} L u_{avg}{}^2} \tag{23}$$

where ΔP is the pressure drop between inlet and outlet flow, u_{avg} is the input average velocity, and L is the axial direction pipe length. ρ_{mix} is the mixture density, $\rho_{crude \; oil}$ is the pure crude oil density, D pipe diameter, ϵ_{mix} is the mixture viscosity. The effectiveness of DRPs can be described in terms of percentage of drag reduction (%Dr) given by the following equations.

$$\%D_r = \frac{\Delta P_{without \; DRA} - \triangle P_{with \; DRA}}{\Delta P_{without \; DRA}} \tag{24}$$

Table 1 Experimental parameters for crude oil pipeline with drag reduction agents

Case	Researchers	Fluid	DRA Type	Concentration. (ppm)	Pipe Dimeter (m)	Length (m)	Flow Rate (m³\hr)
Case A	H.R. Karami, D. Mowla (2013) Ref. [17]	crude oil	mixture from Propylene glycol, Polyolefin synthetic-Ruber,Polyethylene wax	25–200	0.0254 and 0.0127	5.6	1.75–3,98
Case B	Faris et al. (2015) Ref. [8]	crude oil	Naphtha, Toluene	2–10 wt%	0.0318 and 0.0508	3	2–10
Case C	Farhan et al. (2019) Ref. [14]	crude oil	Poly Acrylic Acid (PAA)	50–250	0.0508	5	2.91
Case D	Abdul-hadi, Anees (2013) Ref. [18]	crude oil	SDBS, SLS, SLES and SS	50–250	0.0191, 0.0254, and 0.0508	3	1–12
Case E	H.R. Karami, D. Mowla. Ref. [16]	crude oil	DR1,DR2,and DR3	25–200	0.0254	5.6	1.75–3,98
Case F	Anees. A and Ali. A Ref. [4]	crude oil	Polyacrylamide (PAM)	10–50	0.0254, and 0.0508	3	2–12

Or

$$\%D_r = \frac{f_{crude\ oil} - f_{with\ DRA}}{f_{crude\ oil}} \tag{25}$$

Gyr and Tsinober [37] concluded that DR fluids are essentially non-Newtonian in the turbulent flow region and are usually Newtonian in certain laminar flows. Interestingly, the DR in turbulent flow is considerably higher than that in laminar flow. In pipelines, the turbulent flow occurs as the Reynolds number exceeds 2300. Given that crude oil is a non-Newtonian power-law fluid, the Reynolds number would be determined by the generalized Reynolds number of Metzner and Reed [38] as given below.

$$Re_{MR} = \frac{D^n u_{avg}{}^{2-n} \rho_{mix}}{8^{n-1} k \left(\frac{3n+1}{4n}\right)^n} \tag{26}$$

The Metzner and Reed generalized Reynolds number can be reduced to the conventional Reynolds number by writing it in the following form.

$$Re_{MR} = \frac{\rho_{mix} u_{avg} D}{\mu_{mix}} * C1 * C2 \tag{27}$$

$$Re_{MR} = \frac{\rho_{mix} u_{avg} D}{\mu_{mix}} \left(\frac{D^{1-n}}{8^{n-1} \left(\frac{3n+1}{4n}\right)^n}\right) \left(\frac{u_{avg}{}^{n-1} \cdot k}{\mu_{mix}}\right) \tag{28}$$

Two indexes n and k may define the rheological characteristics of crude oil, thereby representing the flow behaviors and their consistency. When $n = 1$ and $k = \mu$, Equation (27) reduces to the Newtonian fluid Reynolds number given by Equation (21). The rheological characteristics and physical properties of pure crude oil and mixture are listed in Table 2. The apparent viscosity for non-Newtonian crude oil is given by [39]:

$$\mu_{oil} = k \left(\frac{8u_{av}}{D}\right)^{n-1} \tag{29}$$

4.3 Velocity Profile

The velocity profile does not vary in the direction of the flow once the flow is fully developed. Indeed, the shear stress at the wall and pressure gradient are balanced in this region. The distance from the inlet to the starting point of fully developed flow is defined as the entrance length (Le). The entrance

Table 2   Rheological characteristics and properties of pure crude oil and mixture

Case	k	n	Crude Oil Density (kg/m^3)	Crude Oil Viscosity (Pa.s)	Mixture Density (kg/m^3)	Mixture Viscosity (Pa.s)
Case A	0.014	0.748	868	0.0207	870	0.0193
Case B	1.46	0.929	969	0.562	963	0.427
Case C	1.48	0.3	895	0.0275	875	0.016
Case D	–	–	851	0.0021	854	0.00195
Case E	0.014	0.748	868	0.0207	870	0.0193
Case F	–	–	851	0.0041	853	0.0038

length is a function of the pipe diameter, Reynolds number, and the velocity profile for the simulated pipe data was therefore calculated at the entrance length from the following equations [40].

$$\frac{L_e}{D} = 0.06\, R_e \quad \text{for laminar flow,} \tag{30}$$

$$\frac{L_e}{D} = 4.4\, R_e^{1/6} \quad \text{for turbulent flow,} \tag{31}$$

5 Results and Discussion

5.1 Model Validation

As a first step, the validity of the non-Newtonian flow model must be evaluated. Therefore, comparison was made with the experimental data of Karami, H. and Mowla, D. (2013) (Case A). Their results for crude oil experimental data for Pipe 1 (5.6 m length and 0.0254 diameter) at 29°C were taken as a comparison case (Table 3, page 80). Figure 3 shows the simulated friction factor for the $k - \epsilon$ and $k - \omega$ models. An excellent comparison result was obtained between the simulation predictions and the experimental data. In this case, the Reynolds numbers were calculated using Equation (27), and the viscosity of crude oil and mixture viscosity were calculated using Equations (29) and (16) because the rheological properties k and n are listed in their research.

The second validation simulation was performed with H. A. Faris et al. (Case B), in which they used naphtha and toluene as DRAs. First, simulations for crude oil without drag addition were performed with the constant $\Delta B = 0$

Table 3 Simulated Values of friction factor for the at different concentration for Farhan et al. (2019 Ref. [14])

Concentration	$k - \epsilon$ Model			$k - \omega$ Model		
(ppm)	Friction Factor	ΔB	DR%	Friction Factor	ΔB	DR%
0	0.0037221	0	0	0.003550	0	0
50	0.0035214	0.3	5.4000	0.003494	0.3	5.9000
100	0.0033696	0.5	9.4860	0.003342	0.5	8.4000
150	0.0032690	0.7	12.1700	0.003216	0.7	11.2000
200	0.0031489	0.9	15.2000	0.003065	0.9	13.6000
250	0.0029963	1.0	17.1000	0.002972	1.0	16.2000
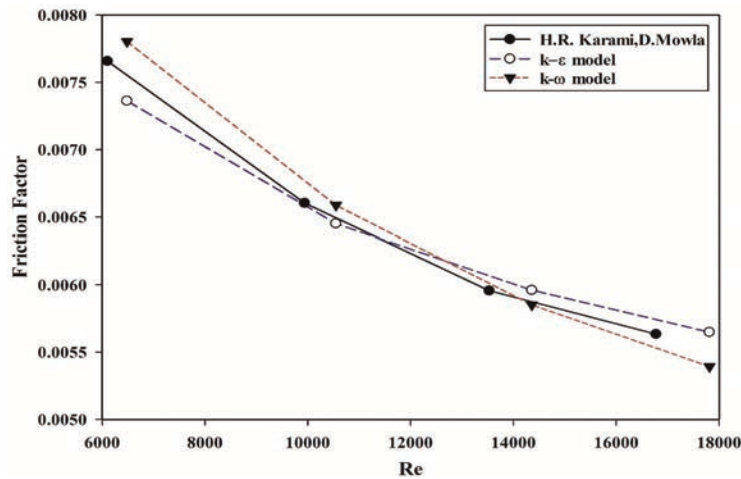
Figure 3 Fiction factor comparison between $k - \epsilon$ and $k - \omega$ models and the experiment data for Karami, H., Mowla, Ref. 17 at various Re.

and $B = 5.2$ in the law of the wall (see e.g. Equation (9)), this value being the one hard-coded in the boundary condition in COMSOL Multiphysics. Then, this value of ΔB was modified to $\Delta B = 2.3$ for crude oil with 10 wt% naphtha or toluene. The $k - \epsilon$ simulation results for the fiction factor for crude oil and crude oil with naphtha as DRA are shown in Figures 4 and 5. The estimated %DR from Equation (24) is plotted and compared with the experimental data of 0.0580 m pipe diameter at 27°C, as shown in Figure 6 for the $k - \epsilon$ and $k - \omega$ models. The predictions for both models show good agreement with the experimental data, especially for the trend of the flow rate and the values of the %DR.
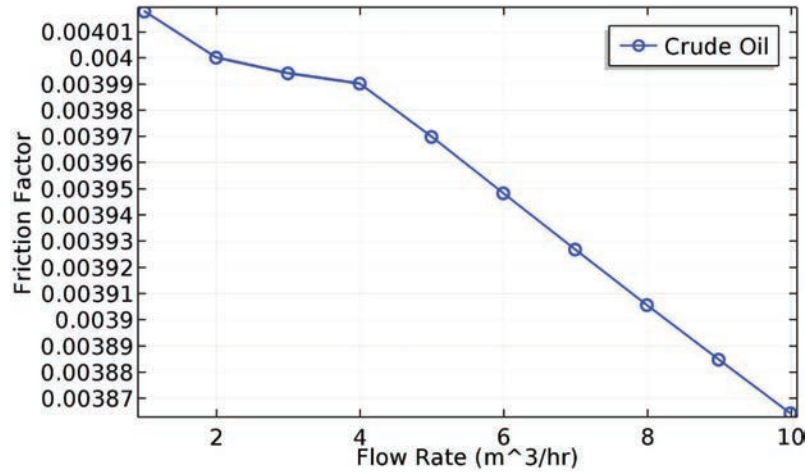
Figure 4   The $k - \epsilon$ simulation results for fiction factor versus crude oil flow rate for Faris et al. (Ref. 8).
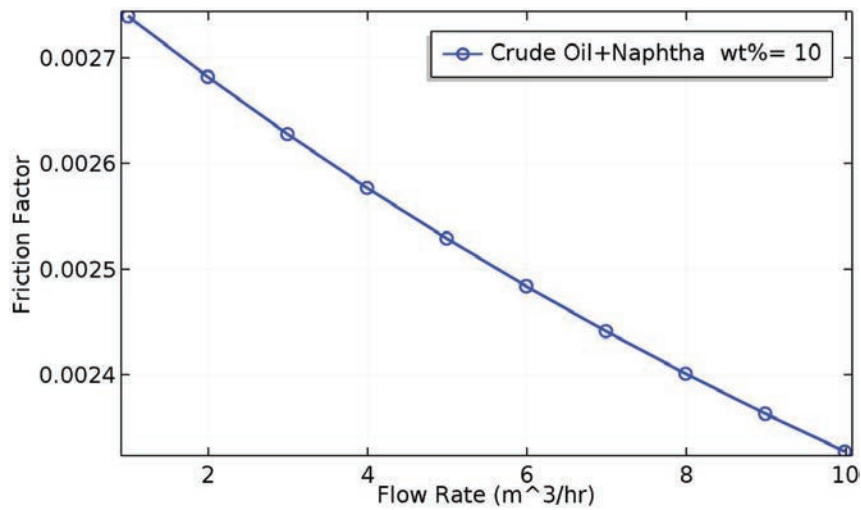

Figure 5   The $k - \epsilon$ simulation results for fiction factor verses crude oil flow rate with 10% Naphtha for Faris et al. (Ref. 8).

5.2 Results of the Models Against Other Cases

In their work (Case C), Farhan et al. examined the performance of poly acrylic acid at different concentrations (0, 50, 100, 150, 200 and 250 ppm)
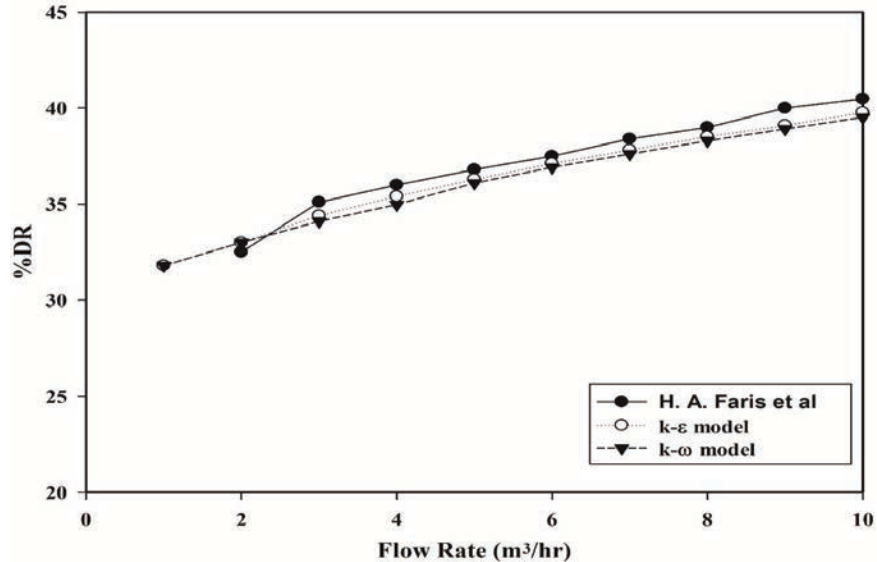
Figure 6 Simulated Drag reduction percentage for crude oil flow rate with 10% Naphtha compared with experimental for Faris et al. (Ref. 8).

for pipeline capacity, pipe diameter and pipe length of 0.00081 m^3/s, 0.0508 m and 5 m, respectively.

In the first step, simulations were conducted with the constant $\Delta B = 0$ in the logarithmic wall law for the $k - \epsilon$ and $k - \omega$ models to determine the friction factor for crude oil without the DRA. Thus, we obtain four computed friction factors (for each DRA concentration), plus the friction factor measured experimentally. Using Equation (24), the %DR is identified at various concentrations for the constant volumetric flow rate. In Figure 7, the predicted data of the %DR is compared with the results of both of models, and the values given by the $k - \epsilon$ model are closer to the experimental data than the $k - \omega$ model. A trial-and-error method were used to determine the best value for the constant ΔB in every simulation runs. That is, different values of ΔB were tried and the predictions for friction factor were compared with the experimental data. Note that each point in Figure 7 has different values of ΔB for each concentration as shown in Table 3.

The influence of four types of surfactants, SDBS, SLS, SLES and SS, on Iraqi crude oil pipelines was investigated by Abdul-hadi and Anees (Case D). To compare the friction factor and %DR for the experimental and simulation results, we chose the surfactant SLES (sodium laureth sulfate) as a case study.
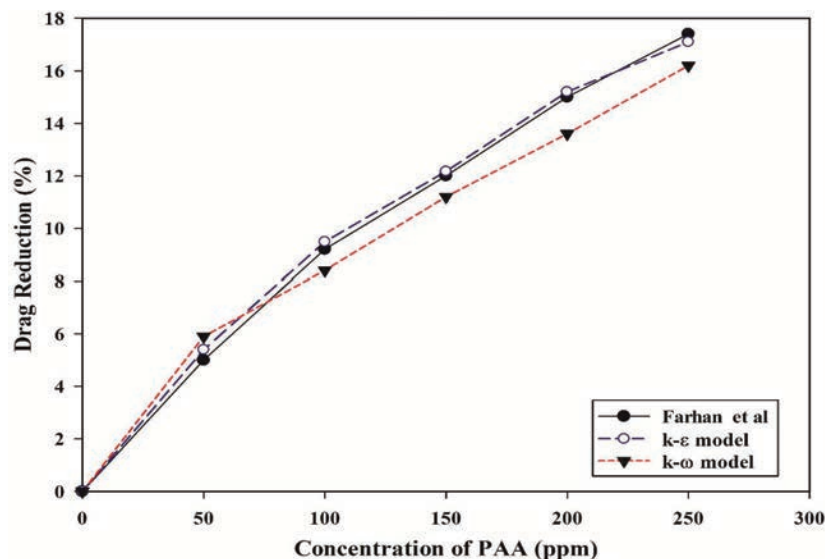
Figure 7   Simulated Drag reduction percentage for crude oil flow rate with different PAA concentration compared with experimental data for Farhan et al. Ref. [14].

Figures 8 ad9 describe the simulated friction factor for 150 ppm of SLES with crude oil flowing inside a 0.0254 m pipe diameter when $\Delta B = 0.2$ for the $k - \epsilon$ and $k - \omega$ models. As can be seen from Figure 10, the estimated values are far from the experimental friction factor at low Reynolds numbers.

The $k - \epsilon$ model seems to perform better in this range. The difference between the numerical and experimental results (Figure 10) arises from both techniques (experimental and numerical). The difference emerges from the uncertainty in the experimental results and in the simplified assumptions in the numerical models. These two inputs can be in the same direction in certain cases and diverge in other cases. Note that a trial method was conducted to minimize this difference by choosing a suitable value of ΔB. Furthermore, the $k - \epsilon$ model gives the most acceptable results and is closest to the experimental data than the $k - \omega$ turbulence model.

The effect of the surfactant concentration on the DR for the 0.0508 m pipe diameter and 12 m³/h flow rate were modelled by changing the ΔB for each concentration. Table 4 demonstrates the simulated data of the friction factor and %DR against the experimental results of Abdul-hadi and Anees (Ref. [18], Figure 2, page 3). A slight difference occurred between the experimental and simulation results for both models.
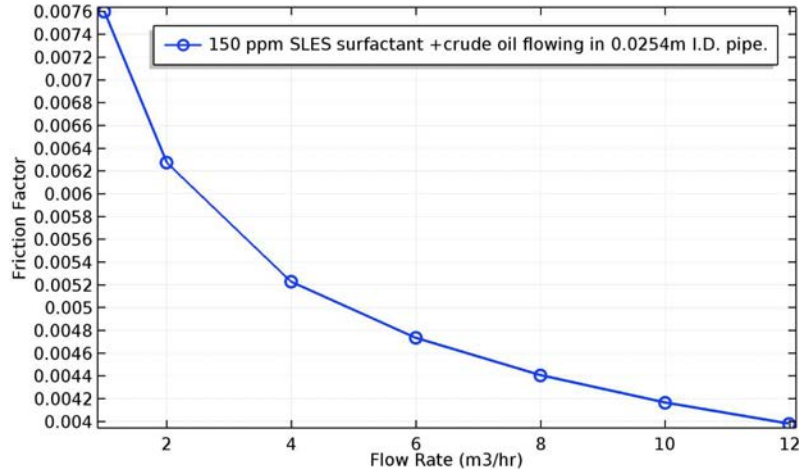
Figure 8 Simulated $k - \epsilon$ friction factor for crude oil flow rate with 150 ppm SLES at different flow rates for Abdul-hadi and Anees, Ref. [18].
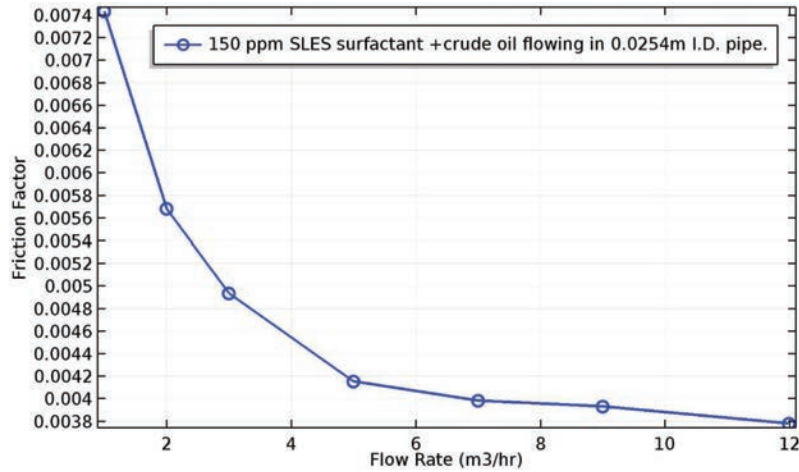

Figure 9 Simulated $k - \omega$ friction factor for crude oil flow rate with 150 ppm SLES at different flow rates for Abdul-hadi and Anees, Ref. [18].

In Case E, Karami, H. and Mowla, D. (2012) studied the effects of using different types of polymers on the crude oil flow in pipelines. Their results for crude oil experimental data for Pipe 1 (5.6 m length and 0.0254 diameter) at 29°C with (25, 50, 75, 100, 150 and 200 ppm) were taken as the case study (Figure 5-a, page 42, in Ref. [16]). Figures 11 and 12 show the simulated $k - \epsilon$
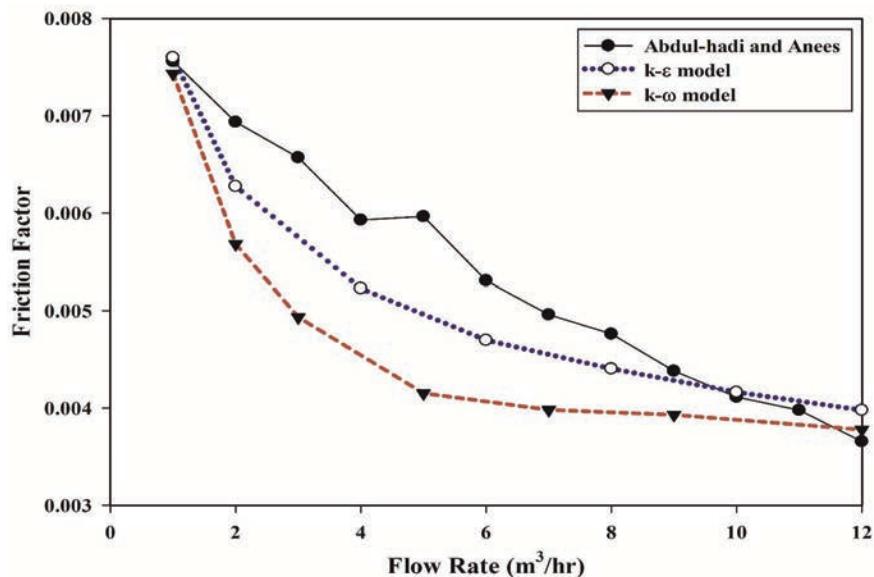
Figure 10   Comparison between $k - \epsilon$ and $k - \omega$ models Fiction factor and the experiment data for Abdul-hadi and Anees, Ref. [18] at different flow rates.

Table 4   Simulated results of friction factor and DR% against the experimental results of Abdul-hadi and Anees, Ref. [18]

Concentration (ppm)	$k - \epsilon$ Model Friction Factor	ΔB	DR%	$k - \omega$ Model Friction Factor	ΔB	DR%	Experimental (Case D) DR%
0	0.0075302	0	0	0.0074168	0	0	0
50	0.0057834	2.8	23.19	0.0057704	2.8	22.20	26
100	0.0054281	4.8	27.92	0.0054285	4.8	26.81	27
150	0.0051066	5.8	32.18	0.0050584	5.8	31.79	32
200	0.0048138	6.3	36.07	0.0047764	6.3	35.60	36
250	0.0045465	6.8	39.62	0.0045249	6.8	39.00	40

and $k - \omega$ friction factors at 150 ppm and $\Delta B = 2.8$. Using Equation (24), the %DR was obtained at different Reynolds numbers, and the friction factor for crude oil ($\Delta B = 0$) is identical to that in Figure 3. Figure 13 shows the typical case for the comparison of the %DR between the experimental and simulated results. As can be seen from the plot, the computed values are far
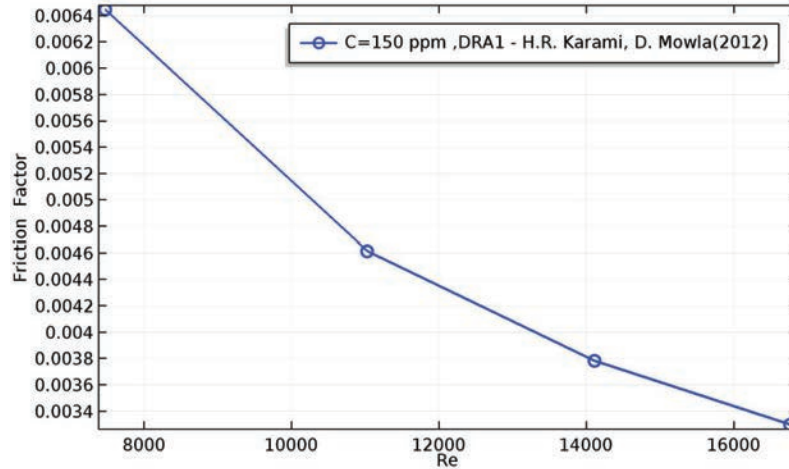
Figure 11   Simulated $k - \epsilon$ friction factor for crude oil with 150 ppm DRA1 at different flow rates for Karami, H., Mowla, D. (2012, Ref. [16]).
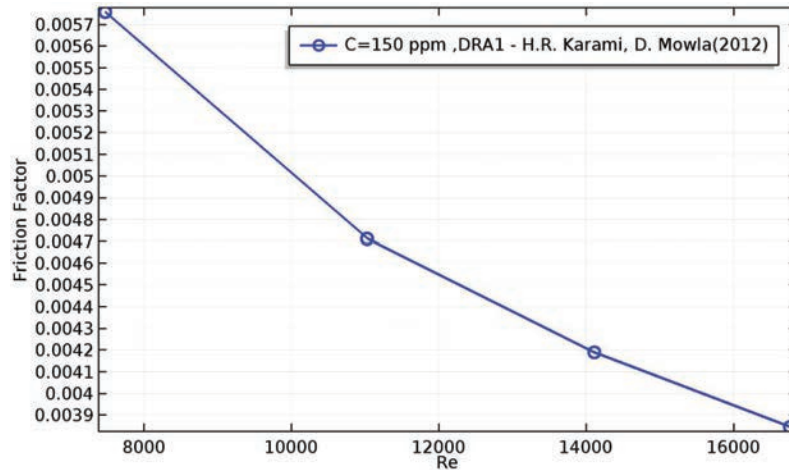

Figure 12   Simulated $k - \omega$ friction factor for crude oil with 150 ppm DRA1 at different flow rates for Karami, H., Mowla, D. (2012, Ref. [16]).

from the measured friction factor. The $k - \epsilon$ model seems to exhibit better agreement at higher Reynolds numbers. For higher Reynolds numbers, the model predicted 41.6% against 38.5% for the experimental results. Clearly, the %DR obtained using the $k - \omega$ model has a lower curvature than the counterpart from using experimental measurements.
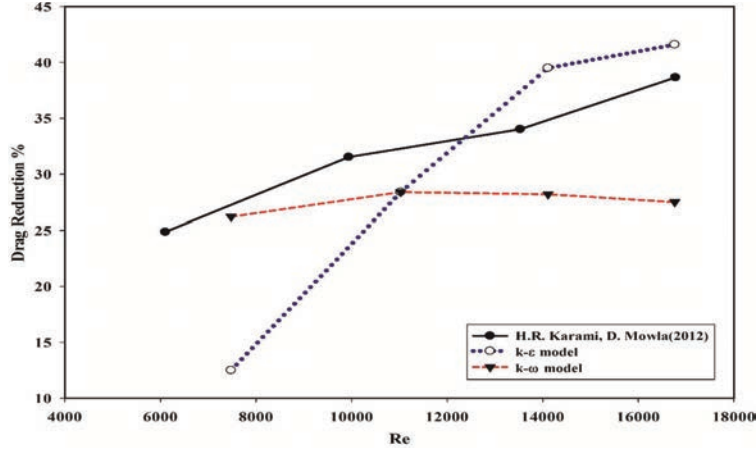
Figure 13   Simulated Drag reduction percentage versus crude oil flow rate with 150 ppm DRA1 compared with experimental data for Karami, H., Mowla, D. (2012, Ref. [16]).

Table 5   Simulated results of friction factor and DR% against the experimental results of H.R. Karami, D. Mowla. Ref. [16]

Concentration (ppm)	$k - \epsilon$ Model			$k - \omega$ Model			Experimental (Case D)	
	Friction Factor	ΔB	DR%	Friction Factor	ΔB	DR%	Friction Factor	DR%
0	0.005647	0	0	0.005393	0	0	0.005633	0
25	0.005296	0.03	6.2	0.005156	0.03	4.39	0.005297	5.95
50	0.004992	0.05	11.6	0.005002	0.05	7.28	0.005082	9.77
75	0.004617	0.06	18.2	0.004688	0.06	13.07	0.004792	14.92
100	0.004290	0.07	24.0	0.004276	0.07	20.71	0.004215	25.17
150	0.003518	1.0	37.7	0.003509	1.0	34.93	0.003456	38.65
200	0.003129	1.3	44.5	0.003151	1.3	41.17	0.003151	44.06

The effect of the DRA1 concentration for 0.0254 m pipe diameter at 29°C and 3.980 m³/h flow rate have been modelled by changing ΔB for each concentration from 0 to 200 ppm. Table 5 provides the simulated data of the friction factor and %DR against the experimental results of Karami, H. and Mowla, D. (2012) (Table 3, page 40 in Ref. [16]). The crude oil friction factors for the $k-\epsilon$ and $k-\omega$ models are 0.005647 and 0.005393, respectively. A slight difference occurred between the experimental and simulation results for both models. Nevertheless, the results obtained from the $k - \epsilon$ model
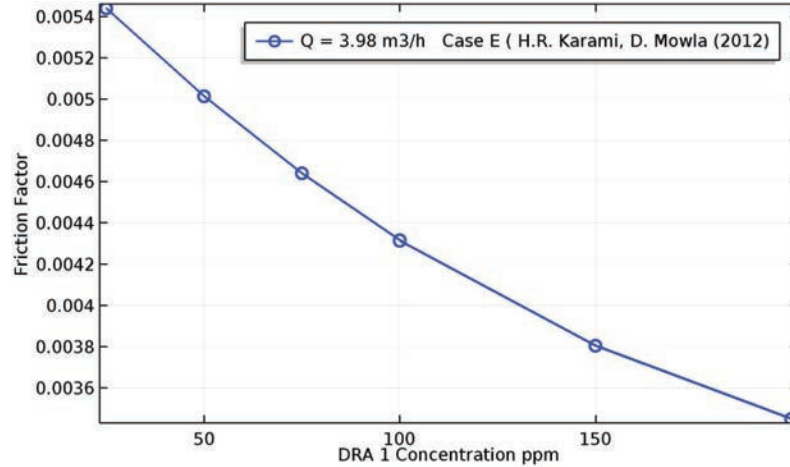
Figure 14   Simulated $k - \epsilon$ model friction factor versus DRA1 concentration at 3.98 m^3/hr for Karami, H., Mowla, D. (2012, Ref. [16]).

Table 6   Simulated results of friction factor and DR% against the experimental results of Anees. A and Ali. A, Ref. [14]

	$k - \epsilon$ Model			$k - \omega$ Model			Experimental (Case D)
Concentration (ppm)	Friction Factor	ΔB	DR%	Friction Factor	ΔB	DR%	DR%
0	0.002984	0	0	0.003304	0	0	0
10	0.002661	1.3	10.81	0.003174	1.3	9.14	12
20	0.002595	1.6	13.03	0.002855	1.6	13.55	13
30	0.002514	1.8	15.75	0.002728	1.8	17.43	15
40	0.002432	2.4	18.53	0.002652	2.4	19.71	18
50	0.002355	2.8	21.06	0.002583	2.8	21.82	21

are closer to the experimental measurements as shown in Table 5. Figure 14 illustrates the simulated $k - \epsilon$ model results when the constant B in the logarithmic velocity law value of 5.2 is set in the simulation models and $\Delta B = 0$. For all concentrations, the simulation model predicts higher values of the friction factor compared to the corresponding experimental and simulation values in Table 6. Figure 14 clearly reveals a strong influence of ΔB in Equation (9) on the friction factor and %DR.
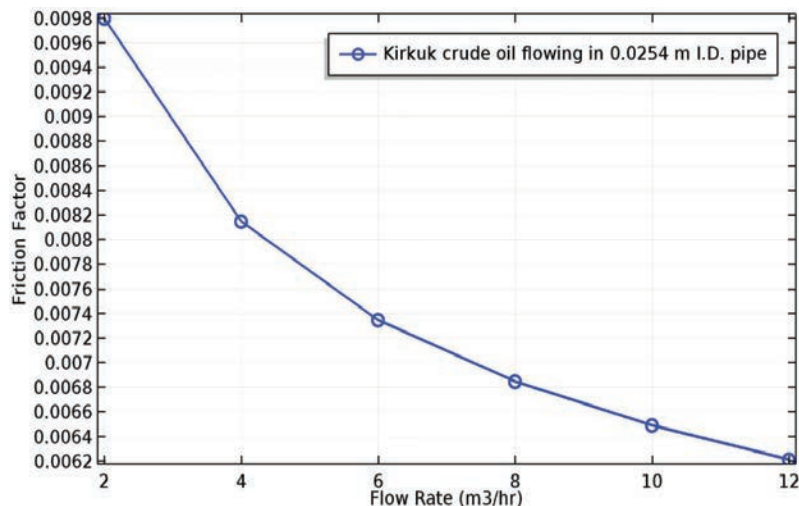
Figure 15   Simulated $k - \epsilon$ model friction factor for crude oil ($\Delta B = 0$) flowing in 0.0254 m dimeter, at different flow rates for Ali A. Abdul-Hadi (2013, Ref. [4].
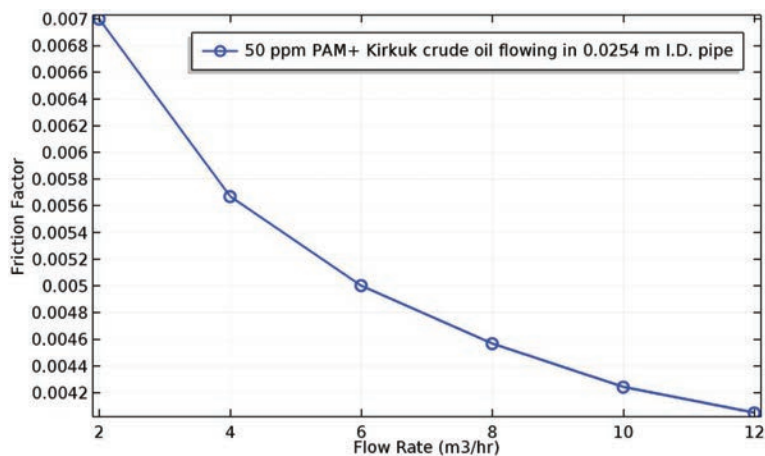

Figure 16   Simulated $k - \omega$ model friction factor for crude oil with 50 ppm PAM ($\Delta B = 0.65$) flowing in 0.0254 m dimeter, at different flow rates for Ali A. Abdul-Hadi (2013, Ref. [4].

In Case F, Anees A. and Ali A. Abdul-Hadi (2013) studied the influence of polyacrylamide (PAM) as a drag reducing polymer on the flow of Iraqi crude oil in pipe lines. Their results for the crude oil experimental data for Pipe 1 (3 m length and 0.0254 m and 0.058 m in diameter) with 10, 20, 30,
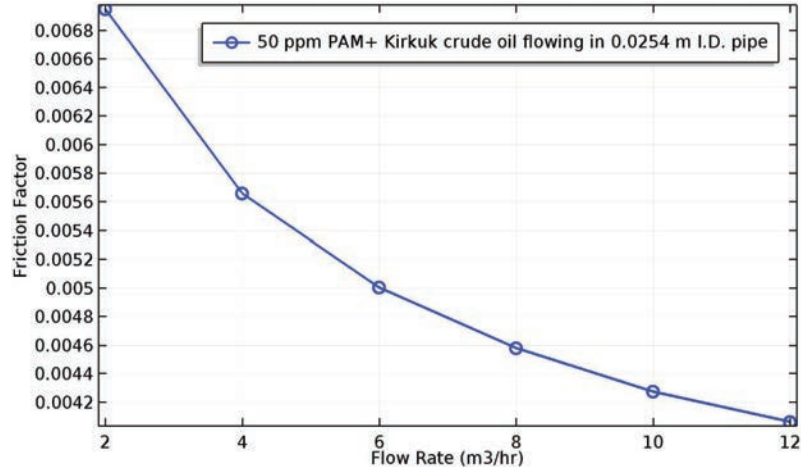
Figure 17   Simulated $k-\epsilon$ model friction factor for crude oil with 50 ppm PAM ($\Delta B = 0.65$) flowing in 0.0254 m dimeter, at different flow rates for Ali A. Abdul-Hadi (2013, Ref. [4]).
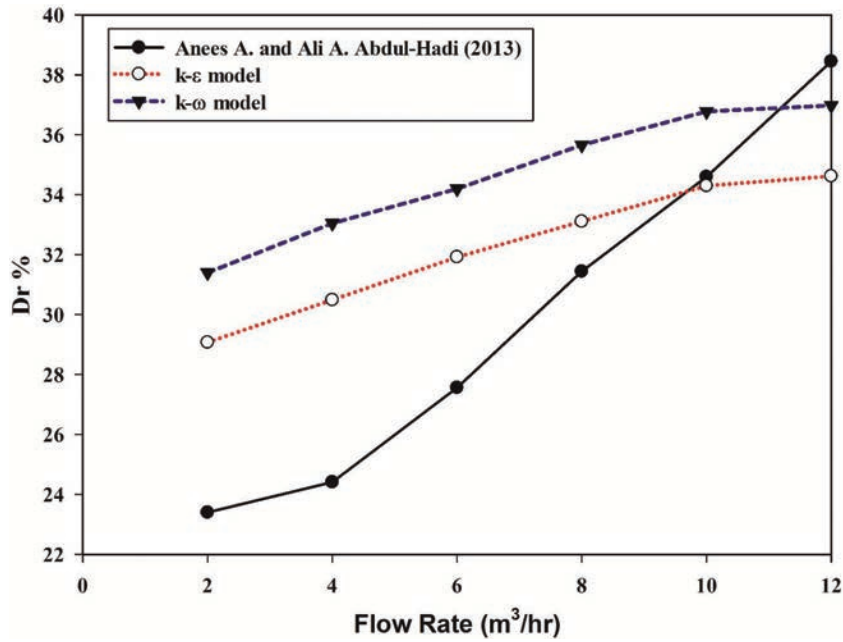

Figure 18   Comparison between $k - \epsilon$ and $k - \omega$ models drag reduction percentage and the experiment data for Anees A. and Ali A. Abdul-Hadi, Ref. [4] at different flow rates.
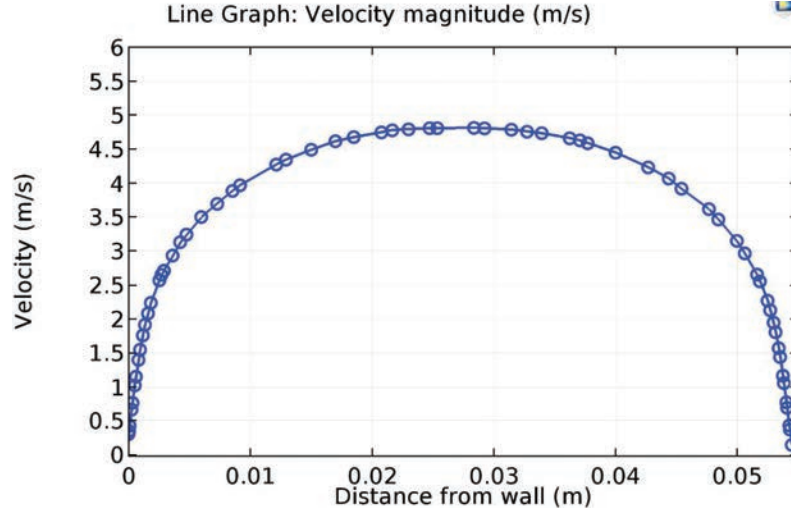
Figure 19   Simulated $k - \omega$ velocity profile at the entrance length for Farhan et al. Ref. [14].

40 and 50 ppm were taken as the case study. Figure 15 shows the simulated $k - \epsilon$ model friction factor for crude oil ($\Delta B = 0$) flowing in 0.0254 m diameter, whereas Figures 16 and 17 show the simulated $k - \epsilon$ and $k - \omega$ models the friction factor for crude oil with 50 ppm PAM ($\Delta B = 0.65$) at different flow rates. Using Equation (24), the %DR was obtained at various Reynolds numbers. Figure 18 reveals the %DR for the $k-\epsilon$ and $k-\omega$ models. The $k-\epsilon$ model seems to achieve better agreement with the experimental data (Table 2, page 3 in Ref. [4]). For all Reynolds numbers, the simulated %DR is greater than the experimental data, but the computed values follow closely follow the measured value at higher flow rates (2–8) m³/hr.

The effect of the PAM concentration for the 0.0508 m pipe diameter and 6 m³/h flow rate have been modelled by changing the ΔB for each concentration. Table 6 presents the simulated data of the friction factor and %DR against the experimental results (Case F). A slight difference occurred between the experimental and simulation results for both models.

5.3 Predicted Velocity Profile and Pressure Drop

Figures 19 and 20 illustrate the Farhan et al. (Case C) velocity profile for fully developed flows at the location determined by Equations (30) and (31) for the $k - \epsilon$ and $k - \omega$ models, respectively. The velocity profile indicates that the velocity at the walls is not zero in the turbulent flow $k - \varepsilon$ simulator.
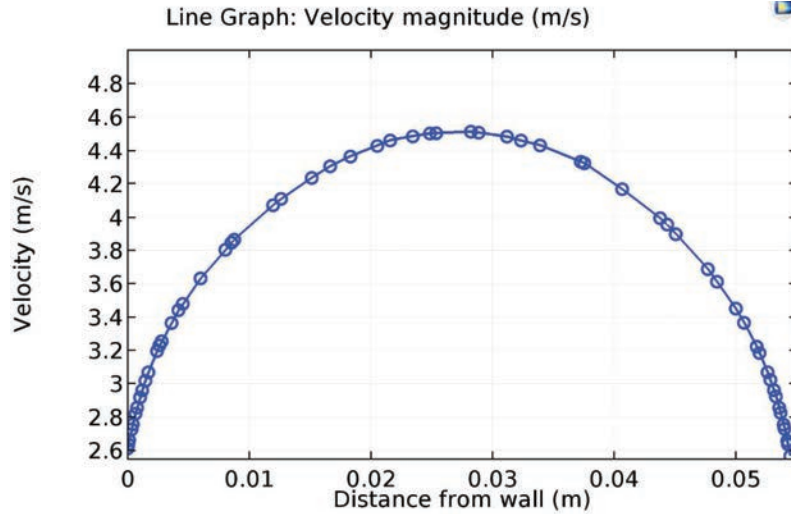
Figure 20   Simulated $k - \varepsilon$ velocity profile at the entrance length for Farhan et al. Ref. [14].
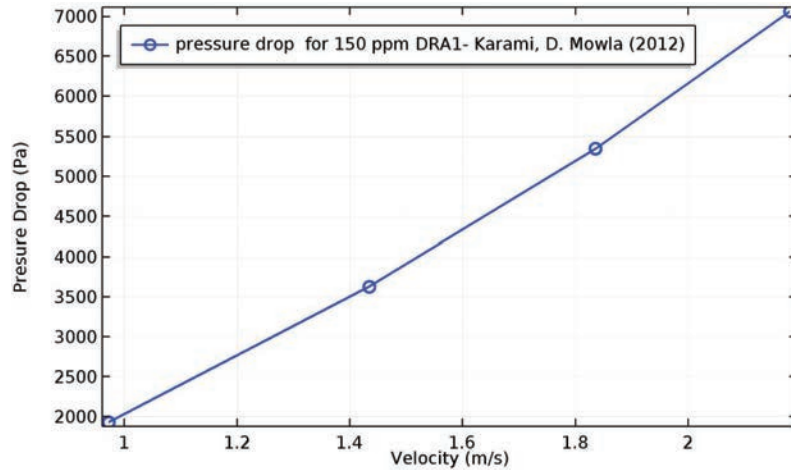
Figure 21   Simulated pressure drop versus velocity for crude oil with 150 ppm DRA1 for H.R. Karami, D. Mowla. Ref. [16].

Therefore, the implementation of the $k - \omega$ model with wall functions can be considered as an effective simulation model for better understanding DR mechanisms because several theories suggest that DR is related to the region near walls. $k - \varepsilon$ model predicts the velocity far from the wall (in the log law zone as shown in Figure 2) and $k - \omega$ model predicts well in the viscous
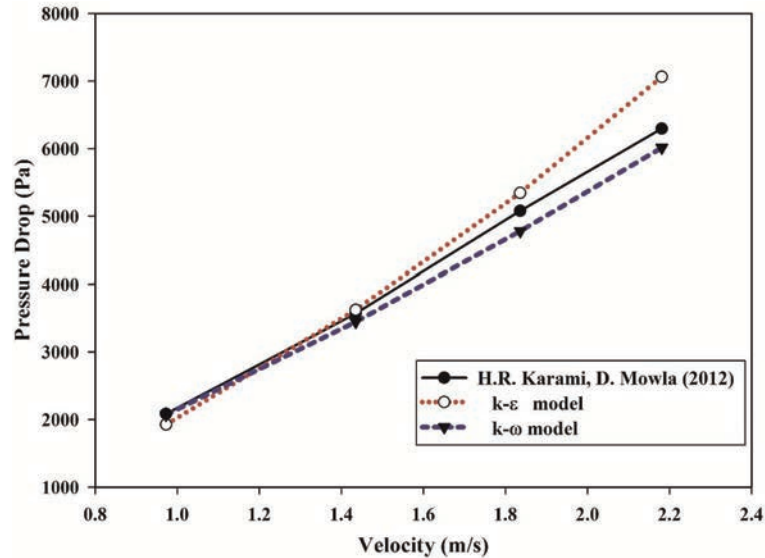
Figure 22   Comparison between $k - \epsilon$ and $k - \omega$ models pressure drop and the experiment pressure drop for H.R. Karami, D. Mowla. Ref. [16].

sublayer near wall. Even though it depends on y^+ and the roughness of the pipe wall. The pressure drop profiles for the fully developed velocity are listed in Case E from H.R. Karami and D. Mowla (2012) for different flow rates, concentrations and lengths. Figure 21 shows the simulated $k - \epsilon$ model for 150 ppm of DRA1 at flow rates ranging from 0.973–2.181 m/s. In Figure 22, the simulated data for $k - \epsilon$ and $k - \omega$ are compared with the experimental results, and the results of the two models are in close agreement with the experimental data (except at a higher range of the Reynolds number).

6 Conclusions

In this work, a numerical study is presented to understand the DR characteristics of the flow of heavy oil flow with different types of DRAs. A series of simulations were used to estimate the friction factor and the %DR and compare the computational results with six experimental research. This study confirms that the $k - \omega$ model has better agreement with experimental results than the $k - \varepsilon$ model in predicting the friction factor and pressure drop for crude oil flow with DR additives. These simulations have shown that both models perform reasonably well relative to the experimental pipe flow results,

with the $k-\omega$ model outperforming the $k-\varepsilon$ model which gives zero velocity at the pipe wall. The models were applied to simulate the flow of crude oil without any additional constitutive equations except changing the constant B to a new value. Moreover, the experimental results are closer to the simulated data, if the constant ΔB in the logarithmic wall law modified to a value greater than 5.2. The friction factor is better predicted by the simulations with $\Delta B = 0$ for crude oil in logarithmic wall law, and its choice depends on the t rheological properties of crude oil and Reynolds number.

References

[1] Brostow, W. Drag Reduction in Flow: Review of applications, Mechanism, and Prediction Journal of Industrial and Engineering Chemistry, Volume 14, 2008, pp. 409–416.

[2] M. H. Hasaean. Studying the Rheological Properties and the Influence of Drag Reduction on a Waxy Crude Oil in Pipeline Flow. Egyptian Journal of Petroleum, 2015, P. 6.

[3] Vejahati, F., A Conceptual Framework for Predicting the Effectiveness of Drag Reducing Agent in Liquid Pipelines. Baltimore, Maryland, Pipeline Simulation Interest Group (PSIG), 2014.

[4] Anees A. Khadom, Ali A. Abdul-Hadi. Performance of Polyacrylamide as Drag Reduction Polymer of crude Petroleum Flow. Ain Shams Engineering Journal, 2014, P. 5.

[5] Al-Amri, N., Al-Khaldi, R., Al-Qahtani, H., Al-Amoudi, M., Multiphase drag reducing agents to increase GOSP production in offshore Saudi Aramco: field applications, Proceeding of The International Petroleum Technology Conference, Doha, 20-22 January, 2014, P. 1–6.

[6] Al-Wahaibi, T., Abubakar, A., Al-Hashmi, A.R., Al-Wahaibi, Y., Al-Ajmi, A., Energy analysis of oil-water flow with drag-reducing polymer in different pipe inclinations and diameters. J. Pet. Sci. Eng. 2017, 149, 315–321.

[7] Eshrati, M., Al-Hashmi, A.R., Al-Wahaibi, T., Al-Wahaibi, Y., Al-Ajmi, A., Abubakar, A.Drag reduction using high molecular weight polyacrylamides during multiphase flow of oil and water: a parametric study. J. Pet. Sci. Eng. 2015, 135, P. 403–409.

[8] Faris, N.A. Samia, A. A. Abdulrazaka, J. S. Sangwaib. The Performance of Toluene and Naphtha as Viscosity and Drag Reducing Solvents for the Pipeline Transportation of heavy Crude Oil, Petroleum Science and Technology Journal, 33:952–960, 2015.

[9] Leighton, R., Walker, D. and Stephens, T. Reynolds Stress Modeling for Drag Reducing Viscoelastic Flows. ASME/JSME 4th Joint Fluids Summer Engineering Conference. American, 2003, 735–744.

[10] Rabie HL, Fouda SM, Awad MM. Turbulence modeling of drag reducing fluid flow using Modified $k - \omega$ model. Fluid Mech Res Int J. 2018; 2(5):219–228.

[11] Pinho, F. T., Li, C. F., Younis, B. A., and Sureshkumar, R. "A Low Reynolds Number Turbulence Closure for Viscoelastic Fluids," J Non-Newton Fluid., 154(2), 2015, pp. 89–108.

[12] Resende, P. R., Kim, K., Younis, B. A., Sureshkumar, R., and Pinho, F. T., "A FENE-P $k - \varepsilon$ Turbulence Model for Low and Intermediate Regimes of Polymer-Induced Drag Reduction," J Non-Newton Fluid., 166(12), 2011, pp. 639–660.

[13] Zheng, Z. Y., Li, F. C. and Li, Reynolds-Averaged Simulation on Turbulent Drag-Reducing Flows of Viscoelastic Fluid Based on User-Defined Function in FLUENT Package. 2014, 14th Joint Fluids Summer Engineering Conference. American.

[14] Farhan Lafta Rashid1, Haider Nadhom, Shaheed Mahdi Talib. Experimental Investigation of Drag Reduction by a Polymeric Additive in Crude Oil Flow in Horizontal Pipe. Journal of Advanced Research in Fluid Mechanics and Thermal Sciences 60, Issue 1 (2019) 15–23.

[15] Al-Kayiem, H., Khan, J. CFD simulation of drag reduction in pipe flow by turbulence Energy promoters. ARPN Journal of Engineering and Applied Sciences, 11, 2016, 14219–14224.

[16] H.R. Karami, D. Mowla. Investigation of the effects of various parameters on pressure drop reduction in crude oil pipelines by drag reducing agents. Journal of Non-Newtonian Fluid Mechanics 177–178 (2012) 37–45.

[17] Karami, H., Mowla, D. A general model for predicting drag reduction in crude oil pipelines, Journal of Petroleum Science and Engineering, 2013, 11, 78–86.

[18] Ali A. Abdul-Hadi and Anees A. Khadom. Studying the Effect of Some Surfactants on Drag Reduction of Crude Oil Flow, Hindawi Publishing Corporation,Chinese Journal of Engineering, Volume 2013, Article ID 321908, 6 pages.

[19] Cindy Dianita, Asep Handaya Saputra, Puteri Amelia Khairunnisa. Simulation of Drag Reducing Polymers for Single and Two Phase Flow in Horizontal Pipe. Journal Rekayasa Kimia dan Lingkungan, 2018, Vol. 13, No. 2, pp. 154–164.

[20] Strelnikova, S., Michkova, D. Mathematical modeling of fluid motion in pipelines using drag reducing agents, Proceeding of PSIG Annual Meeting, Prague, 2013, 16–19 April, 1–12.

[21] Zhang, X., Duan, X., Muzychka, Y. (2018). Analytical Upper Limit of Drag Reduction with Polymer Additives in Turbulent Pipe Flow. Journal of Fluids Engineering, 140(5).

[22] Wilcox, D. C., 1998. Turbulence Modeling for CFD, 2nd edition. DCW Industries, Inc., La Canada, California.

[23] Wilcox, D. C., 2006. Turbulence Modeling for CFD, 3nd edition. DCW Industries, Inc., La Canada, California.

[24] Virk PS. Drag reduction fundamentals. AICHE J 1975; 21:625–656.

[25] Schlichting, H., Gersten, K., (2000). Boundary-Layer Theory. Springer-Verlag, Berlin, Heidelberg, New York.

[26] Benzi, R., Ching, E. S. C., Horesh, N. & Procaccia, I. 2004a Theory of concentration dependence in drag reduction by polymers and the maximum drag reduction asymptote. Phys. Rev. Lett. 92(7), 078302.

[27] Yang, S. Q. & Dou, G. 2005 Drag reduction in flat-plate turbulent boundary layer flow by polymer additive. Phys. Fluids 17 (**??**), 065104

[28] Yang, S. Q. & Dou, G. 2008 Modelling of viscoelastic turbulent flow in open channel and pipe Phys.Fluids 20 (**??**), 06510.

[29] Yang, Shu-Qing & Dou, Guo-Ren. (2008). Modeling of viscoelastic turbulent flow in channel and pipe. Physics of Fluids - PHYS FLUIDS. 20. 10.1063/1.2920275.

[30] Xin Zhang, Xili Duan, Yuri Muzychka, Zongming Wang. Experimental correlation for pipe flow drag reduction using relaxation time of linear flexible polymers in a dilute solution. The Canadian Journal of Chemical Engineering. Volume 98, Issue 3, March 2020, P. 792–803.

[31] COMSOL Multiphysics. Chemical Engineering Module, User's Guide. COMSOL AB, 2012.

[32] Sellin et al. (2008). The effect of drag-reducing additives on fluid flows and their industrial applications part 1: basic aspects. Journal of Hydraulic Research 20, No 1.

[33] H. Nourozieh, M. Kariznovi, J. Abedi, Viscosity measurement and modeling for mixtures of Athabasca bitumen/hexane. Journal of Petroleum Science and Engineering. 129 (2015) 159–167.

[34] Lederer, E.L. (1933) Proc. World Pet. Cong. (Lond.) 2, 526–528.

[35] Shu, W.R. (1984) A Viscosity Correlation for Mixtures of Heavy Oil, Bitumen and Petroleum Fractions. SPE 11280.

[36] Saeed Mohammadi, Mohammad Amin Sobati, and Mohammad Taghi Sadeghi. Viscosity Reduction of Heavy Crude Oil by Dilution Methods: New Correlations for the Prediction of the Kinematic Viscosity of Blends. Iranian Journal of Oil & Gas Science and Technology, Vol. 8 (2019), No. 1, pp. 60–77.

[37] Gyr, A., and Tsinober, A. (1997). On the rheological nature of drag reduction phenomena. J. Non-Newtonian Fluid Mechanics 73:153–162.

[38] Metzner, A.B., Reed, J.C., 1955. Flow of non-Newtonian fluids-correlation of the laminar, transition and turbulent-flow regions. AIChEJ. 1, 434–440.

[39] Kané, M., Djabourov, M. and Volle, J. L., (2004), Rheology and structure of paraffinic crude oils in quiescent and under shearing conditions. Fuel, 83(11,12): 1591–1605.

[40] Munson, B. R., Young, D. F., & Okiishi, T. H., Fundamentals of Fluid Mechanics, 4th Ed., New York: John Wiley and Sons, Inc, 2002

Biographies

Ali Nasir Khalaf received his B.Sc. and M.Sc. degrees in Chemical Engineering from Basrah University-Engineering College, and Ph.D. degree in Mechanical Engineering from University of Basrah – College of Engineering, Iraq. Dr. Khalaf a faculty member at the College of Engineering – University of Basrah since 1992.

Asaad. A. Abdullah received his B.Sc. and M.Sc. degrees in mechanical Engineering from University of Basrah – College of Engineering, Iraq; and Ph.D. degree in Mechanical Engineering from the Huazhong University of Science and Technology, China. Dr. Abdullah, a faculty member at the College of Engineering – University of Basrah since 2002.